

See discussions, stats, and author profiles for this publication at: <https://www.researchgate.net/publication/261799756>

Fermi Resonance as a Tool for Probing Peridinin Environment

ARTICLE in THE JOURNAL OF PHYSICAL CHEMISTRY B · APRIL 2014

Impact Factor: 3.3 · DOI: 10.1021/jp501667t · Source: PubMed

CITATIONS

6

READS

59

9 AUTHORS, INCLUDING:



Daniele Bovi

Sapienza University of Rome

13 PUBLICATIONS 90 CITATIONS

SEE PROFILE



Leonardo Guidoni

Università degli Studi dell'Aquila

90 PUBLICATIONS 1,436 CITATIONS

SEE PROFILE



Bruno Robert

Atomic Energy and Alternative Energies Com...

192 PUBLICATIONS 6,094 CITATIONS

SEE PROFILE



Riccardo Spezia

Université d'Évry-Val-d'Essonne

109 PUBLICATIONS 1,059 CITATIONS

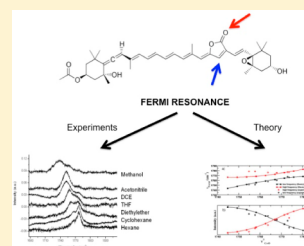
SEE PROFILE

Fermi Resonance as a Tool for Probing Peridinin Environment

Elizabeth Kish,[†] Maria Manuela Mendes Pinto,[†] Daniele Bovi,[‡] Marie Basire,^{§,||} Leonardo Guidoni,[⊥] Rodolphe Vuilleumier,^{§,||} Bruno Robert,^{*,†} Riccardo Spezia,^{*,@} and Alberto Mezzetti^{*,†,#}[†]Institut de Biologie et de Technologie de Saclay, CEA, and UMR 8221, CNRS, Bat 532, CEA Saclay, 91191 Gif/Yvette, France[‡]Dipartimento di Fisica, "La Sapienza" Università di Roma, P.le Aldo Moro 5, 00185 Rome, Italy[§]Département de Chimie, Ecole Normale Supérieure, 24, rue Lhomond, 75005 Paris, France^{||}UPMC Univ Paris 06, UMR 8640 CNRS-ENS-UPMC, 4, Place Jussieu, 75005 Paris, France[⊥]Dipartimento di Scienze Fisiche e Chimiche, Università degli studi dell'Aquila, Via Vetoio, Coppito, 67100 L'Aquila, Italy[@]CNRS, LAMBE UMR 8587, Université d'Evry-Val-d'Essonne, 91025 Evry Cedex, France[#]LASIR UMR 8516, Université Lille I Bat. C5, Cité Scientifique, 59655 Villeneuve d'Ascq, France

S Supporting Information

ABSTRACT: In the present paper, we provide an extended study of the vibrational signature of a butenolide carotenoid, peridinin, in various solvents by combining resonance Raman spectroscopy (RRS) with theoretical calculations. The presence of a Fermi resonance due to coupling between the lactonic C=O stretching and the overtone of the wagging of the C–H in the lactonic ring provides a spectroscopic way of differentiating between peridinins lying in different environments. This is a significant achievement, given that simultaneous presence of several peridinins (each with a peculiar photophysical role) in different environments occurs in the most important peridinin containing proteins, the peridinin-chlorophyll proteins (PCPs) and the Chl *a*-c2-peridinin binding proteins. In RRS, small modifications of solvent polarity can give rise to large differences in the intensity and splitting between the two bands, resulting from the Fermi resonance. By changing the polarity, we can tune the frequency of stretching of the C=O and, while the C–H wagging frequency is almost always constant in different solvents, move the system from a perfect resonance condition to off-resonance ones. We have corroborated our spectroscopic findings with a quasi-classical dynamical model of two coupled oscillators, and DFT calculations on peridinin in different solvents; we have also used calculations to complete the peridinin vibrational mode assignments in the 800–1600 cm^{−1} region of RRS spectra, corresponding to polyene chain motion. Finally, the presence of Fermi resonance has been used to reinterpret previous vibrational spectroscopic experiments in PCPs.



1. INTRODUCTION

Carotenoids represent one of the most widespread groups of naturally occurring pigments, which are largely responsible for the red, yellow, and orange color of fruits, vegetables, flowers, and a wide range of organisms. Characteristically, carotenoids contain alternating carbon–carbon single and double bonds, from which arise their electronic properties that confer them various functions in biology, ranging from light-harvesting and energy dissipation to protection against singlet oxygen.¹

One carotenoid molecule in particular, peridinin (Per), is found in the light harvesting complexes of dinoflagellates, both in the water-soluble peridinin-chlorophyll-proteins (PCPs) and the membrane-bound Chl *a*-c2-peridinin binding proteins.² PCPs have received considerable attention in the last 15 years (reviewed in ref 3), given the availability of high-resolution structures derived from X-ray crystallography,⁴ their peculiar photophysical behavior,^{3,5} their use as a fluorophore in biomedical research,^{3,6} and as a light-harvesting element in nanostructures for light energy conversion.^{3,7} Furthermore, artificial PCPs (with simpler structure and/or different chlorophylls) can also be produced by mixing the apoprotein

with exogenous pigments,^{3–5} making these proteins ideal systems to investigate energy transfer mechanisms.

In contrast to other chlorophyll-protein complexes, soluble PCPs have carotenoid molecules that outnumber the chlorophylls (the normal ratio is 4:1).^{2,3} The structure of the PCP complexes consists of two symmetric domains, each with a central chlorophyll (in naturally occurring PCPs, Chl *a*), usually surrounded by four Per molecules.⁴ The protein provides distinctive surroundings for the pigment molecules, and in PCPs, each Per displays different absorption properties, suggestive of different functions for these pigments within the protein.^{3,5}

The molecular structure of Per shows several peculiar features: instead of the C₄₀ structure characteristic of most carotenoids, Per has an unusual C₃₇ skeleton; an allene moiety and a butenolide ring are conjugated with the π system of the carotenoid backbone.^{3,5} An ester group is located on one β -ring with a tertiary alcohol, whereas an epoxy group with a

Received: February 16, 2014

Revised: April 18, 2014

Published: April 22, 2014

secondary alcohol is located on the opposite β -ring (the Per structure is shown in Figure 1). The allene and butenolide

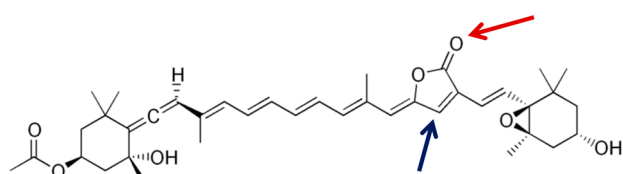


Figure 1. Peridinin structure. The two chemical moieties whose vibrational modes (stretching and out-of-plane wagging, respectively) are coupled by Fermi resonance are put in evidence. The lactonic C=O is indicated by the red arrow, whereas lactonic C–H is indicated by the blue arrow. See text for further details.

moieties have been shown to be crucial in determining the peculiar photophysical characteristics of Per, notably the presence of a S_0 – S_1 transition (which is normally forbidden in carotenoids by symmetry), which explains its relatively high fluorescence quantum yield.^{3,5} The presence in the excited state potential energy surface of a so-called intramolecular charge transfer (ICT) state is stabilized in polar solvents and is further enhanced in protic solvents through hydrogen bonding involving the butenolide C=O of Per as an acceptor.^{3,5,8–10}

The vibrational band associated with the lactonic C=O stretching has been largely used as a probe to study Per and PCP photophysics.^{11–17} In particular, the dependence of the position of the carbonyl stretching bands on the environment has been proposed¹⁶ as a rationale to distinguish between the lactonic C=O stretching bands of different Pers in PCPs during singlet–singlet Per–Chl energy transfer^{11,13} or upon triplet state formation.^{12,14,15} The different mechanisms by which the surrounding environment can modulate the position of the lactonic C=O band of Per has recently been investigated by our groups¹⁶ by performing vibrational

spectroscopy (Raman and Infrared) experiments on Per in different solvents coupled to QM/MM molecular dynamics simulations, which provide a molecular rationale of the observed behavior. We found that the position of the lactonic C=O stretching band is strongly environment-dependent. Its position can vary between 1735 and 1777 cm^{-1} , with two key factors influencing band shape and position: the dielectric constant of the solvent and the involvement of the lactonic C=O in a hydrogen bond (as an acceptor) with the solvent.¹⁶ In ref 16, just three solvents were used, following a typical rationale of an apolar solvent (cyclohexane), a polar/aprotic solvent (acetonitrile), and a polar/protic solvent (methanol).

In this work, Per vibrational spectra have been studied in a wider range of solvents for further investigation of the lactonic carbonyl band, using resonance Raman spectroscopy (RRS) and theoretical calculations. RRS is an excellent tool to study carotenoids;¹⁸ as a vibrational technique, it yields direct information about the properties of the molecule's electronic ground state.

2. MATERIALS AND METHODS

Sample Preparation. Per was extracted from main-form PCP (MFPCP) from *Amphidinium carterae*. Pigments of MFPCP were extracted with butanol,¹⁹ dried under vacuum, and dissolved in ethanol. Per was separated from the crude pigment extract using a Strata C-18-E (55 μm , 500 mg/6 mL) column (Phenomenex). The sample was applied in 70% of Strata Solution (StS: 50% methanol/50% acetonitrile) followed by a wash step [70% StS for two column volumes (CV)]. Per was eluted by application of 95% StS, dried under vacuum, and shipped at room temperature for further experiments.

Solvents. The solvents used were tetrahydrofuran (THF), hexane, cyclohexane, and acetonitrile (all absolute grade, $\geq 99.5\%$ GC), 1,2-dichloroethane (DCE), methanol (anhydrous, 99.8%), and diethyl ether ($\geq 99.8\%$ GC), all purchased from

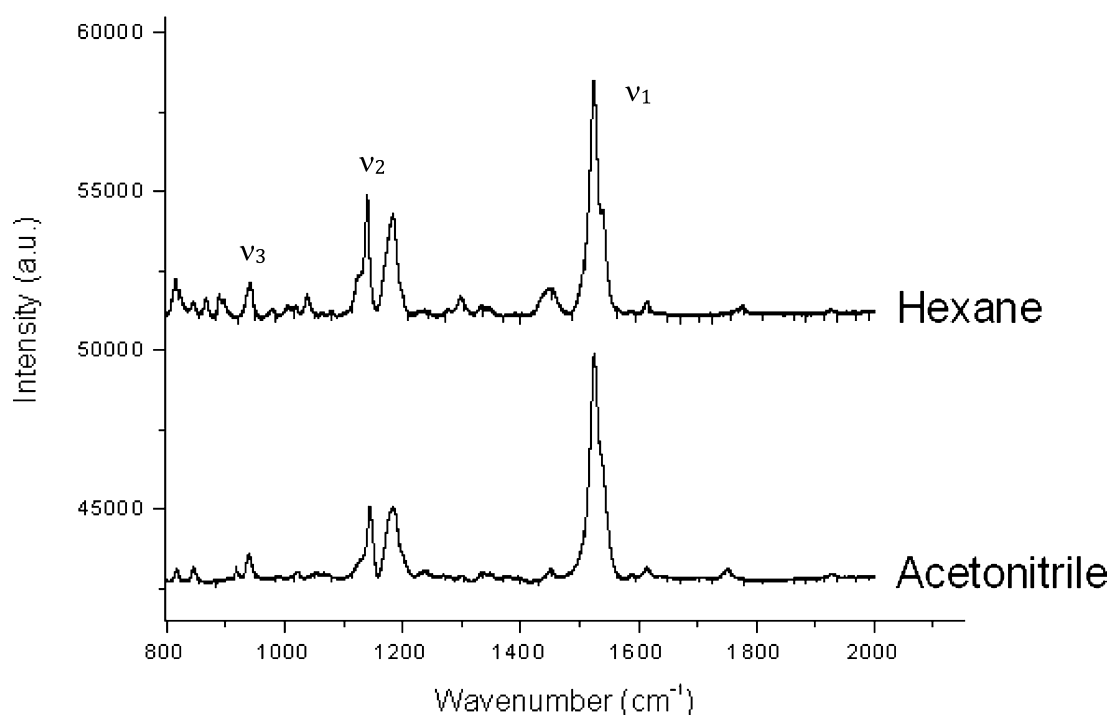


Figure 2. Resonance Raman spectra of peridinin in *n*-hexane and acetonitrile (excitation wavelength 514.5 nm, spectral window 800–2000 cm^{-1}).

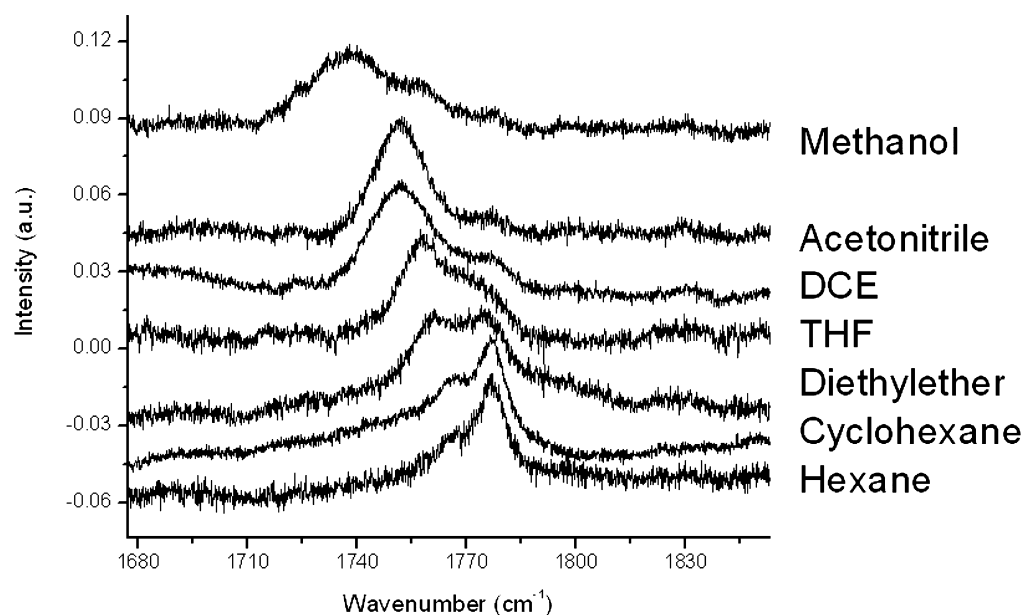


Figure 3. Resonance Raman spectra of peridinin (excitation wavelength of 514.5 nm, spectral window of 1680–1840 cm^{-1}) in different solvents.

Sigma-Aldrich (St. Louis, MO). Solutions with Per were freshly prepared and measured immediately; exposure to light and oxygen was avoided.

Spectroscopy. Room temperature UV–vis absorption spectra of Per dissolved in the different solvents were measured in a 1 cm optical path length quartz cuvette using a Varian Cary ES double-beam scanning spectrophotometer, and optical density was between ~ 0.2 and 0.4 OD.

RRS was performed on Per in seven solvents with an excitation wavelength of 514.5 nm; supplementary experiments were carried out for three solvents (cyclohexane, diethyl ether, and acetonitrile) using 488.0, 496.5, and 501.7 nm excitation wavelengths. Excitation was provided by a 24 W Ar^+ Sabre laser (Coherent, Palo Alto, California), and spectra were recorded at room temperature with 90° signal collection using a two-stage monochromator (U1000, Jobin Yvon, Longjumeau, France), equipped with a front-illuminated, deep-depleted CCD detector (Jobin Yvon, Longjumeau, France). In order to prevent sample degradation by the absorbed light, low intensity laser power (typically less than 20 mW) reached the sample during recording of the spectra, and sample integrity was systematically assessed by following the evolution of the resonance Raman (RR) spectra during the experiment. Absorption UV–vis spectra were also taken before and after the RRS experiment to ensure there was no sample degradation. Spectra were collected between 800 and 2000 wavenumbers (cm^{-1}).

For each measured spectrum, at least three spectra were collected and averaged; and other treatment was done on the spectra, such as removal of peaks due to cosmic waves or dead detector pixels. A multipoint baseline was taken and spectra were normalized according to the ν_1 peak. Peak positions were determined, considering second derivatives of the recorded spectra.

The FTIR spectrum of solid Per was recorded on a Bruker Tensor 22 spectrometer equipped with an Attenuated Total Reflectance accessory and a DTGS detector.

DFT Calculations. DFT calculations were performed on the complete Per molecule (Figure 1). The system is relatively

large, since it has a C_{37} carbon skeleton for an overall size of 96 atoms. The DFT calculations were performed using the ORCA package,^{20,21} with the GGA functional PBE²² in the spin-restricted Kohn–Sham scheme. The TZVP Ahlrichs basis sets²³ have been employed for all atoms with the SCF convergence defined “TightSCF” (energy change of 1×10^{-8} ; max-density change of 1×10^{-7} ; rms density change of 5×10^{-9} ; and DIIS error of 5×10^{-7}), and a high precision for the integration grids (“Grid4”) is used. The minimum energy geometry calculation and the vibrational analysis were performed in different solvents using the implicit solvation approach COSMO.²⁴

3. RESULTS AND DISCUSSION

Figure 2 displays the RR spectrum of Per obtained at 514.5 nm excitation in hexane and acetonitrile (i.e., in solvents of different polarity). Three main groups of bands can be observed, termed ν_1 to ν_3 . Typical of carotenoids, the ν_1 band at 1524 cm^{-1} mainly arises from the stretching modes of the $\text{C}=\text{C}$ double bonds.²⁵ The shoulder of this band at higher frequency (also attributed to a normal mode located on the $\text{C}=\text{C}$ chain²⁵) is slightly more pronounced as solvent polarity decreases (data not shown). Generally in carotenoids, the so-called ν_2 band comprises a main component and two to three satellites.²⁶ In Per, three bands are observed (at ~ 1125 , ~ 1140 , and $\sim 1180 \text{ cm}^{-1}$). We attribute the ν_2 peak at $\sim 1140 \text{ cm}^{-1}$ to coupling between the in-plane rocking vibrations of the methyl groups attached to the conjugated chain with the adjacent $\text{C}-\text{H}$ in-plane bending modes. A small but significant solvent effect is observed for this band, which shifts from 1140 cm^{-1} (in hexane) to 1145 cm^{-1} (in acetonitrile). DFT calculations actually predict that a band arising from the $\text{C}-\text{C}$ single bond stretching modes coupled with $\text{C}-\text{H}$ in-plane bending modes (ν_2) shifts about 6 cm^{-1} when transferring Per from hexane to acetonitrile (see Table S1 of the Supporting Information). This suggests that the mode becomes a bit more localized on the polar part of the molecule when moving to a more polar solvent. The ν_3 band in Per appears at around 940 cm^{-1} , which corresponds to a lower frequency value as compared to most carotenoid molecules, for which this band is usually observed

Table 1. Resonance Raman Experimental Values of ν_a and ν_b peaks, Corresponding to the C=O Stretching Spectral Region for Different Solvents^a

	Dielectric Constant (ϵ_r)	High Frequency Peak Position ν_a	High Frequency Peak Intensity	Low Frequency Peak Position ν_b	Low Frequency Peak Intensity
acetonitrile	37.5	1778.0	0.006	1751.7	0.043
methanol	32.7	1778.0	0.008	1737.7	0.031
DCE	10.4	1778.0	0.013	1751.4	0.041
THF	7.6	1776.1	0.020	1757.5	0.039
diethyl ether	4.3	1775.7	0.032	1759.8	0.031
cyclohexane	2.0	1776.9	0.043	1767.3	0.029
hexane	1.9	1776.9	0.035	1766.1	0.015

^aFrequencies are in wavenumbers (cm^{-1}), and intensity is in arbitrary units. Note that the reported position of the ν_b band in methanol is due to the Per conformer involved as an acceptor in a hydrogen bond with the solvent (see text for further details). Solvent dielectric constants (ϵ_r) are also reported.

around 1000 cm^{-1} . In β -carotene, the ν_3 band is mainly attributed to rocking modes of the methyl group of the carotenoid chain.²⁵ At 940 cm^{-1} , β -carotene also has a peak, termed ν_4 , which involves the C–H out-of-plane wagging motions coupled with C=C torsional modes, which are out-of-plane twists of the carbon backbone.²⁵ This mode is not coupled with the electronic transition for planar molecules and gains intensity upon distortions of the conjugated chain; it is used as a reporter of the carotene planarity.^{26,27} Experimentally, a small increase in the frequency value is observed from Per in acetonitrile to hexane/cyclohexane (from 939 to 942 cm^{-1}). The frequency of the corresponding C–H out-of-plane wagging mode in our DFT calculations (see Table S1 of the Supporting Information) is slightly decreased, when changing from polar to nonpolar solvent. This experimentally observed relatively small effect (3 cm^{-1} upshift) cannot be therefore described by the static DFT calculations, which also do not take into account the RR intensities.

In the high frequency region of these spectra (around 1750 cm^{-1}), there is a weaker band (compared to ν_1 , ν_2 , and ν_3) arising from the stretching modes of the Per conjugated lactonic C=O group (Figure 3).¹⁶ As expected from the stretching modes of a bond possessing a large intrinsic dipole, these modes are highly sensitive to the polarity of the solvent (Table 1) and display a global downshift in spectra of Per in hydrogen bond-donating solvents like methanol (Figure 3, Table 1), due to the formation of H bond(s) between the methanol OH group (donor) and the Per lactonic carbonyl (acceptor). Surprisingly, two peaks may be observed in every solvent in this spectral region. If we exclude the H-bond-donating solvent methanol, a peak around 1777 cm^{-1} (hereafter called ν_a) is present in every solvent, together with another peak whose position is solvent dependent and varies between 1751.4 and 1767.3 cm^{-1} (hereafter called ν_b) (see Table 1 and Figure 3).

Per indeed possesses two different carbonyls: the lactonic one and an ester carbonyl. However, the latter is nonconjugated and, hence, is not expected to contribute to the RR spectra. Furthermore, the frequency of the stretching mode of this C=O, as previously observed,¹⁶ is expected at lower wavenumbers.

The two C=O stretching frequencies (ν_a and ν_b) could reflect inhomogeneity in our samples. However, the RR spectra we obtained in different solvents allow us to rule out the presence of *cis* Per isomers in our samples. Carotenoid isomerization, by playing on the molecular symmetry, induces the appearance of additional modes in the RR spectra, which

are not observed here.²⁸ Furthermore, DFT calculations predict that, as expected, such *cis*–*trans* isomerizations should not affect C=O frequencies by more than a few wavenumbers (not shown). Finally, even if such a difference in the C=O stretching value existed, the two C=O peaks corresponding to two different isomers would shift in parallel, following the solvent polarity.

We cannot hastily rule out other sources of inhomogeneity in our samples, arising either from the Per sample or our solvents. However, if a subpopulation of Per in our sample would differ by its interactions with the solute, it should display a slightly different absorption spectrum (see Figure S1 of the Supporting Information). The Per absorption spectrum is indeed particularly sensitive to the molecule environment.^{5,8,9} Thus, we completed a series of experiments using three solvents (cyclohexane, diethyl ether, and acetonitrile), which span the range of dielectric constants, using a range of excitation wavelengths (488.0 , 496.5 , 501.7 , and 514.5 nm). In general, we do not observe any wavelength dependence in the Per RR spectra (Figure 4 displays the lactonic carbonyl region of Per in the different solvents as an example).

In Per, it is now well-established that an ICT state exists in this excited state manifold.^{3,5,8–10} Presence of this state could induce different resonance conditions, depending on whether or not the excitation wavelength matches with the S_0 to S_1 /ICT transition. However, such change in resonance would be expected to affect primarily the intensity of the C=O stretching mode and not its frequency (which primarily depends on the ground-state electronic structure). Moreover, the absence of large excitation wavelength dependence in our spectra (see Figure 4) indicates either that the resonance with the S_1 /ICT transition is much weaker than with S_2 or that none of the excitation wavelengths used in this study match with the energy of this transition.

We are thus led to conclude that the presence of two stretching frequencies in the Per RR spectra is an intrinsic property of Per itself, and more precisely, of its lactonic C=O. The presence of two peaks associated with the C=O stretching has actually already been described for other unsaturated lactones,^{29–33} and this effect has been generally interpreted in terms of a Fermi resonance between C=O stretching of the lactone moiety (the “fundamental peak”, red arrow in Figure 1) and the out-of-plane (oop) wagging of the C–H on the lactonic ring (whose overtone lies in the same spectral region as the C=O stretching; the involved C–H is indicated by the blue arrow in Figure 1).³⁴ The fundamental mode of the lactonic C–H oop wagging should be in the 884 – 887 cm^{-1}

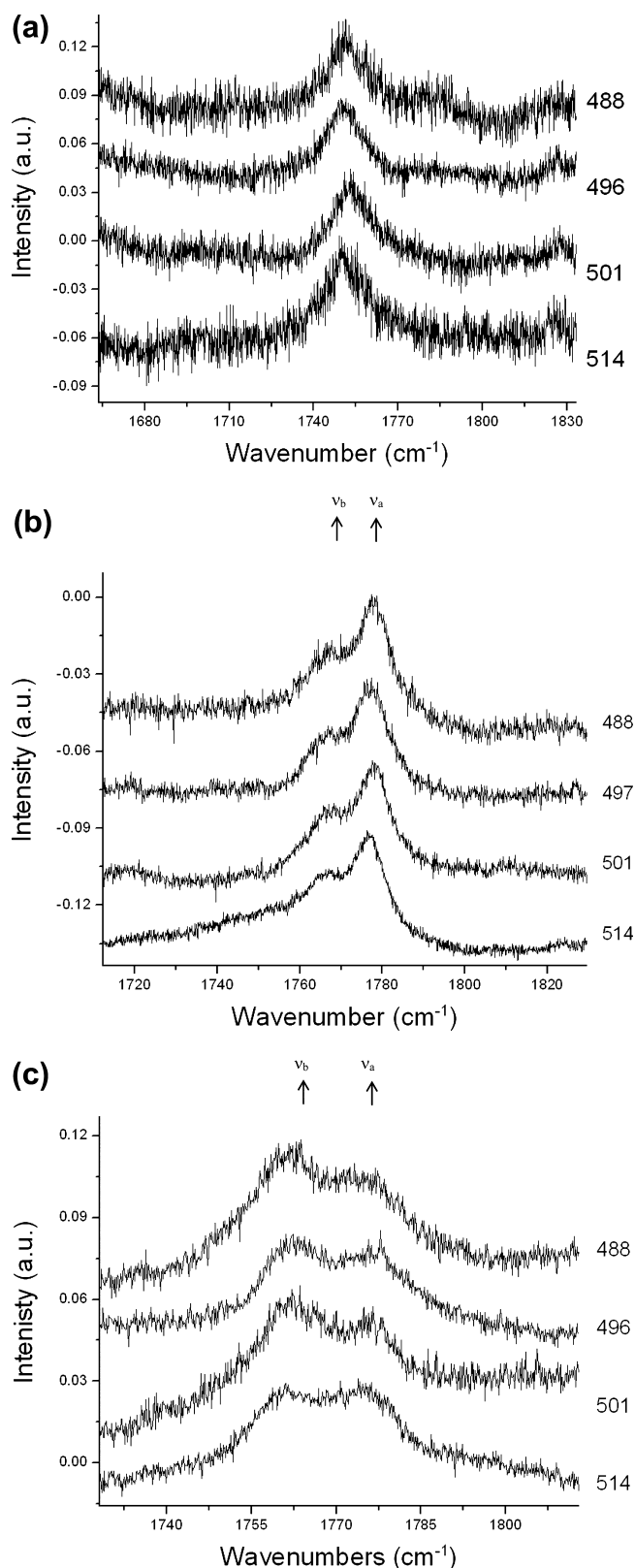


Figure 4. Resonance Raman spectra at different wavelengths in the carbonyl region. The solvents are (a) acetonitrile, (b) cyclohexane, and (c) diethyl ether.

region, since this is half of the frequency of the signal that we observe (all overtones are double the frequency of the fundamental mode). However, the peak in this range should

not be present in our RR spectra, since the lactonic C–H oop wagging mode is not coupled with electronic transitions involving the π -electron conjugated systems, when the molecule is planar. The FTIR spectrum of solid Per shows IR bands between 870 and 900 cm⁻¹ (Figure 5). These data, along

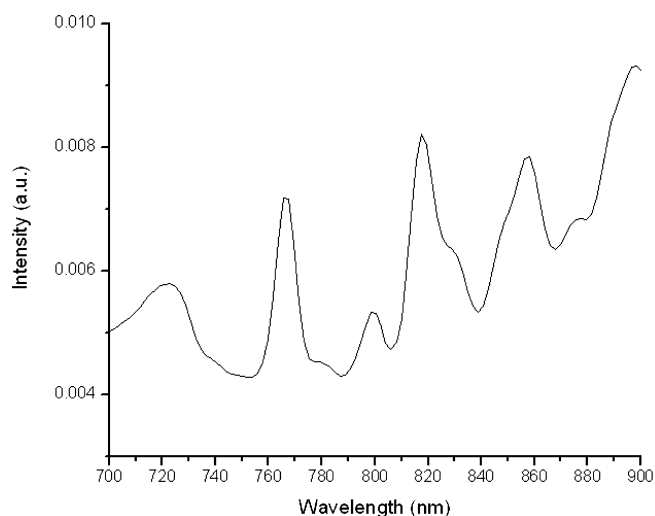


Figure 5. FTIR spectrum of solid Per in the 700–900 cm⁻¹ region.

with DFT calculations on normal modes of Per strongly support that the lactonic C–H oop wagging lies in, or very close to, the 884–887 cm⁻¹ range. The C=O band splitting observed by the 514.5 nm RRS experiments in different solvents could thus come from intrinsic vibrational properties of the system. The Fermi resonance should be in turn tuned by solvent polarity, which modulates the C=O frequency.

Two different kinds of theoretical calculations were performed to check the validity of this Fermi resonance model, where the resonance is tuned by solvent polarity. First, DFT calculations showed that the lactonic C=O stretching frequency largely decreases as the solvent polarity increases (as could be expected from the simple consideration that polarity reduces the double bond character, see Figure 6a). On the other hand, the lactonic C–H oop wagging modes are nearly constant in all the solvents investigated (see Figure 6b). We can therefore draw the following picture combining DFT with

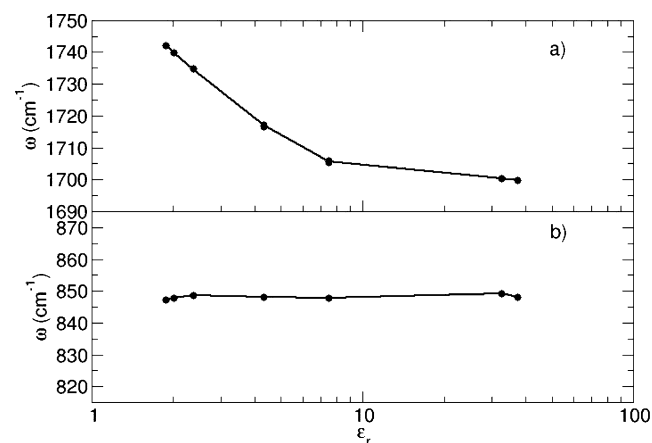


Figure 6. DFT frequencies (unscaled values) corresponding to C=O stretching (panel a) and C–H wagging (panel b) as a function of solvent dielectric constant, ϵ_r .

experimental results: for very apolar solvents, the C=O stretching frequency is slightly higher than the lactonic C–H oop wagging overtone. When the solvent polarity increases, the C=O stretching lowers its frequency; for diethyl ether, which has a dielectric constant (ϵ_r) of 4, we have perfect resonance (equal intensity between ν_a and ν_b in RR spectra). By further increasing the solvent polarity, the C=O and the C–H oop wagging overtone become more and more off-resonance and the high frequency peak, ν_a , becomes lower and lower in intensity. (The limit for acetonitrile: $\epsilon_r = 37.5$; in this case, ν_a appears just as a weak shoulder).

The second theoretical approach we used relies on the usual model to explain Fermi resonance (i.e., the coupling between two harmonic oscillators):

$$V(x_1, x_2) = \frac{1}{2}\omega_1^2 x_1^2 + \frac{1}{2}\omega_2^2 x_2^2 + \frac{1}{2}\gamma x_1 x_2^2 \quad (1)$$

where x_1 and x_2 are mode positions away from equilibrium (equilibrium is taken as the spectrum from diethyl ether), ω_1 and ω_2 are the corresponding frequencies, and γ the coupling. In the case of Per, the first mode corresponds to the high frequency C=O stretching and the second to the low frequency lactonic C–H oop wagging. The coupling form, $1/2 \gamma x_1 x_2^2$, is the same originally proposed by Fermi, discussing for the first time such resonance in the Raman spectrum of CO₂.³⁵ However, in the present case only one low frequency mode has been considered; it is also Raman inactive. The coupling value was obtained from the spectrum of Per in diethyl ether, where the intensities of ν_a and ν_b are equal with the incident wavelength of 514.5 nm; from the frequency difference, we can evaluate a coupling value of 15 cm⁻¹.

Then, we have generated quasi-classical trajectories where the initial conditions were obtained by a Wigner sampling³⁶ of the uncoupled Hamiltonian (i.e., the Hamiltonian of two oscillators employing potential of eq 1 where $\gamma = 0$) at 298 K and then propagated by numerically solving the classical Newton equation of motion on the full Hamiltonian, using a standard velocity Verlet algorithm.³⁷ For each system, we have propagated an ensemble of 10000 trajectories for about 100 ps. Then, power spectra were obtained from the Fourier transform of the full velocity–velocity correlation function (vibrational density of states, VDOS). Note that the spectra will be composed by both active and inactive Raman (and/or IR) modes, since our model does not include dipole moments or polarizability. Here we focus our attention on the high-energy mode that corresponds to the C=O vibration and on the position and intensity of the two peaks resulting from the coupling (i.e., the resonance).

On the basis of the picture arising from experiments and DFT calculations, we employ the Fermi resonance model (eq 1) to obtain positions and intensities of the peaks using different values of “uncoupled” C=O, $\nu_{C=O}^0$ (ω_1 in eq 1), while the ω_2 value was kept constant ($\omega_2 = 883.5$ cm⁻¹, i.e., $2\omega_2 = \omega_1$). Note that the uncoupled value corresponds to the frequency that would result if no coupling between modes was present. These values were then used as the input parameters for the calculations. The results are shown in Figure 7, where we have assumed, based on experimental results, perfect resonance at 1767 cm⁻¹ (two peaks of the same intensity) and span the uncoupled C=O frequency from 1745 to 1780 cm⁻¹. These C=O frequencies correspond to tuning solvent polarity. On the other hand, as zeroth-order approximation, the coupling was considered unchanged over the whole frequency range. In

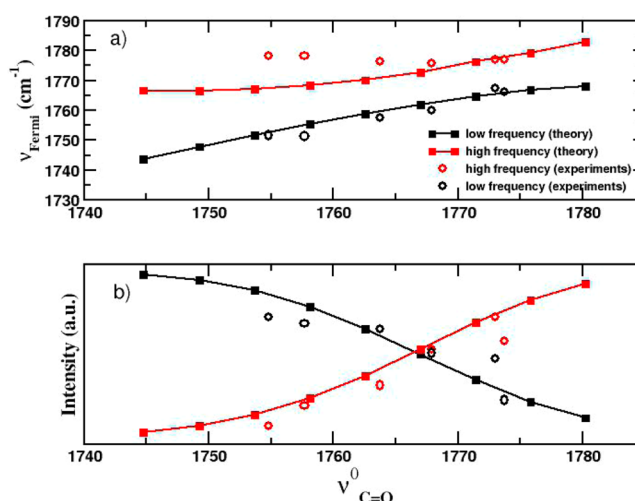


Figure 7. The frequency (upper panel) and intensity (lower panel) of the two peaks obtained from quasi-classical dynamics (full circles and solid lines), employing the Fermi resonance model (eq 1) at different values of the uncoupled C=O stretching frequency ($\nu_{C=O}^0$). The high-frequency peak (ν_a) is in red, and the low frequency (ν_b) is in black. In open circles, we show experimental values obtained by using eq 2 on the RRS data.

the same figure, we have added results obtained from experiments. Note that experiments provide the two frequencies ($\nu_{C=O}$) and intensities for the series of solvents used but not the C=O frequencies ($\nu_{C=O}^0$) if they were not coupled (we need these values to compare experimental and theoretical results). To obtain the uncoupled $\nu_{C=O}^0$ values from experiments, we have used the simple formula,³⁰ derived from perturbation theory applied to a Fermi resonance coupling between a fundamental frequency and an overtone (eq 1):

$$\nu_a^0 = \frac{(\nu_a + \nu_b)}{2} + \frac{(\nu_a - \nu_b)}{2} \left[\frac{I_a - I_b}{I_a + I_b} \right] \quad (2)$$

where ν_a and ν_b are the experimental peak positions and I_a and I_b are the corresponding relative intensities. Experimental and theoretical points are in relatively good agreement concerning intensities, which is surprising due to (1) the simplicity of the model and (2) the fact that the source of intensity in VDOS and RR spectra are very different (VDOS gives purely dynamical information and RRS implies polarizability changes and excited states). Concerning the frequencies of the two peaks, we found a good agreement between experiments and calculations, in particular for the low frequency (ν_b) resonant peaks (black points in Figure 7, panel a). Some differences are obtained in the position of high frequency (ν_a) resonant peaks (red points in Figure 7, panel a), in particular for low frequency off-resonance portion (i.e., points for which $\nu_{C=O}^0$ is lower than 1767 cm⁻¹). It seems that the experimental data reach a plateau before theoretical points. This can be due to the fact that we have considered the perfect resonance value as 1767 cm⁻¹; shifting it to higher frequencies could recover a similar plateau (note that theoretical calculations show that ν_a reaches a plateau, just at lower frequencies than experiments). Unfortunately, experimentally the higher frequency corresponds to the less polar solvent available, so we cannot verify the behavior at higher frequencies. We should also keep in mind that the 1767 cm⁻¹ value was taken from RR intensities (i.e., from the

spectrum from which we have almost identical RR intensities, the one of Per in diethyl ether), while our theoretical model is based on pure vibrational density of states (VDOS). Furthermore, some other approximations, like fixing the coupling value across the frequency range and having considered only one low-frequency mode coupled to the C=O stretching, could be the origin of this slight difference between calculated and experimental values.

Despite these small discrepancies, overall the calculated spectra are in good agreement with the experimental results, thus reinforcing our hypothesis of Fermi resonance.

4. RELEVANCE TO BIOPHYSICAL STUDIES

The results described above clearly show that the lactonic C=O of Per is extremely sensitive to its surrounding environment (because of the solvent dielectric constant and hydrogen bonding), as suggested before.¹⁶ In addition, due to the Fermi resonance effect, even small variations in the dielectric constant of the surrounding environment can be probed by the lactonic C=O. It has already been pointed out¹⁶ that the lactonic C=O of each Per in MFPCP from *A. carterae* can be “classified” as a C=O in a polar/protic environment (“methanol-like”), in a polar but aprotic environment (“acetonitrile-like”), or in an apolar/aprotic environment (“cyclohexane-like”). With the new data presented in this paper, two new pieces of information can be derived: (a) the Fermi resonance makes it possible to distinguish between Per, whose C=O lie in environments with a difference in ϵ_r of 2 or less, in apolar/aprotic environments. Relying just on our previous work,¹⁶ such distinction was a priori not possible; as in those cases, the simple effect of the dielectric constant around carbonyls on the position of the lactonic C=O stretching band is not strong enough. With the present results, thanks to the extremely high dependence of the Per Fermi resonance effect on the dielectric constant (particularly evident for apolar environments), these Per carbonyls can now, in principle, be distinguished spectroscopically. It is difficult to propose here a qualitative classification (e.g., “diethyl-ether-like” environment vs “DCE-like” environments) of the same kind of that proposed in ref 16, as in this case the parallelism between the solvent environment in solutions and pigment–protein interactions in protein binding pocket is not as appropriate as in ref 16. Nevertheless, the basic ideas remain: the perfect resonance is for a dielectric constant (around the lactonic C=O) of ~ 4 ; for more polar environments, the ν_a band is more intense than the ν_b , and for less polar environments, the ν_b band is more intense than the ν_a . (b) As a consequence of the Fermi resonance, if two (or more) bands in the lactonic C=O region are observed in a vibrational spectrum of Per-containing proteins (or more broadly speaking, Per-containing systems), this does not necessarily imply that these bands arise from more than one Per. It should be emphasized that, given that a weak Fermi resonance takes place also in quite polar environments, this phenomenon should always be taken into account. In the following, we will analyze some results from the literature.

Bonetti et al. reported¹⁴ in a ³Per/Per step-scan FT-IR difference spectrum in THF, a negative peak for the lactonic C=O of Per at 1761 cm⁻¹; however, their spectrum clearly shows a shoulder at ~ 1776 cm⁻¹, in agreement with our RR spectrum of Per in THF, shown in Figure 3. Step-scan FT-IR difference spectra at 298 K in MFPCP^{15,17} and PCP from *Heterocapsa pygmaea*,¹⁴ where ³Per formation is expected, show, among others, several negative bands in the lactonic carbonyl

region. For all excitations used, negative bands are observed above 1760 cm⁻¹.^{15,17} Two carotenoid triplet states were identified in MFPCP, and both are associated with negative vibrational contributions above 1760 cm⁻¹, which could arise from Fermi resonance. This is, in particular, the case for a negative peak at ~ 1770 cm⁻¹, associated with the fast-decaying triplet state,^{14,15,17} whose position matches our RR observations.

Step-scan FT-IR difference spectra at 100 K on MFPCP,¹² contrary to the spectra recorded at 298 K, did not show any clear trace of negative bands above 1760 cm⁻¹, which could possibly reflect Fermi resonance for the lactonic C=O of (one or more) Per(s). This, however, is most probably related to a modification of the triplet formation mechanism, as suggested by other spectral features.¹² Conversely, these 100 K step-scan FT-IR difference spectra show, beside the expected positive band at 1719 cm⁻¹ (attributed to the lactonic C=O stretching of ³Per), a positive band at 1766 cm⁻¹. This seems to suggest that a Fermi resonance effect may also be present for the lactonic C=O of (one or more) ³Per.

Ultrafast IR spectra¹¹ on MFPCP recorded with a 480 nm excitation also show negative bands at 1770 and 1749 cm⁻¹, which were assigned to Per. The low spectral resolution of the data does not allow for their detailed analysis, but the presence of these two bands most probably reflects a Fermi resonance effect for the lactonic ring of Per. It is worth noting that the ultrafast IR data published on PCP¹¹ (as well as the data on Per in organic solvents^{11,13}) also show two or more positive peaks in the carbonyl region. This seems to suggest that Fermi resonance for the lactonic C=O may also be present when Per is in the S₁/S_{1CT} state.

Outside the domain of PCP photophysics, it should be noted that the sensitivity of the Per C=O vibration band to the surrounding environment may provide a way to investigate the biological role of Per (see, for instance, ref 38) at a molecular level. This role is probably related to the presence, and to the biochemical action, of the unsaturated lactonic ring, as observed for similar butenolide compounds.³⁹

The observed Fermi resonance between the lactonic C=O and the C–H oop wagging of the lactonic ring is also expected to take place in Per derivatives, such as peridinol, anhydroperidinol, and peridin-3'-ester, given that the lactonic moiety lies in the conjugated chain. In literature, values for the lactonic C=O stretching are also reported for other butenolide carotenoids in solid state (e.g., pyroxanthin acetate⁴⁰). Also for these molecules, under opportune conditions, Fermi resonance involving the lactonic C=O is expected to take place. Also, as previously mentioned, the occurrence of a Fermi-resonance induced double peak for the C=O stretching has been reported for other simpler butenolide compounds.^{29–33} This suggests that the role of the polyene chain in the Fermi resonance effect observed for Per is somehow marginal. Indeed, the investigation of vibrational mode localization in Per,¹⁶ already pointed out that, despite the conjugation between the polyene chain and the lactonic carbonyl, the normal mode of vibration associated with the lactonic carbonyl stretching is almost exclusively localized on the C=O.

It is therefore very likely that Fermi resonance takes place also in other naturally occurring butenolides. Possibly, this effect can be exploited in the investigation of the interaction of these molecules with their environment to better understand their biological role.

5. CONCLUSIONS

In this paper, we report a detailed characterization of the environmental effects on the vibrational properties of Per, notably on the lactonic C=O stretching band, by using organic solvents as model systems. In particular, we have shown that in aprotic environments, a strong Fermi resonance effect takes place and a clear explanation for its dependency on the dielectric constant of the medium has been presented. The vibrational spectroscopy literature results obtained on PCPs have been re-examined in the light of this new effect, which has so far been underestimated in the analysis of vibrational spectra. In particular, the Fermi resonance may make it possible to distinguish among Pers having their lactonic C=O lying in very similar, but not identical, binding sites in PCPs as well as in other Per-containing proteins. In addition, the same effect has been previously shown to take place also in other butenolide molecules. It is therefore likely that the same approach, the possible appearance of C=O twin bands arising from Fermi resonance, whose effectiveness is modulated by the interaction between the lactonic C=O and its environment, may be used also in biophysical investigations on other biologically relevant butenolides.

■ ASSOCIATED CONTENT

Supporting Information

Vibrational frequencies, ν_2 and ν_3 , of peridinin as obtained by DFT calculations in different solvents (unscaled frequencies) are shown in Table S1; UV-vis absorption spectra of peridinin in different solvents are reported in Figure S1. This material is available free of charge via the Internet at <http://pubs.acs.org>.

■ AUTHOR INFORMATION

Corresponding Authors

*E-mail: bruno.robert@cea.fr.

*E-mail: riccardo.spezia@univ-evry.fr.

*E-mail: alberto.mezzetti@univ-lille1.fr.

Notes

The authors declare no competing financial interest.

■ ACKNOWLEDGMENTS

We thank Dr. Tim Schulte and Dr. E. Hoffman from the Ruhr-Universität Bochum for purifying and sending us peridinin for our experiments. Financial support from European Research Council (Advanced Grant PHOTOPROT n. 267333) is greatly acknowledged. This work was supported by the French Infrastructure for Integrated Structural Biology (FRISBI) ANR-10-INSB-05-01.

■ REFERENCES

- (1) *Carotenoids: Natural Functions*; Britton, G.; Liaaen-Jensen, S.; Pfander, H., Eds.; Birkhäuser: Basel, Switzerland, 2008; Vol. 4.
- (2) Macpherson, A. N.; Hiller, R. G. Light-Harvesting Systems in Chlorophyll c-Containing Algae. In: *Light-Harvesting Antennas in Photosynthesis*; Green, B. R., Parson, W. W., Eds.; Kluwer Academic Publishers: Dordrecht, The Netherlands, 2003; pp 323–352.
- (3) Carbonera, D.; Di Valentin, M.; Spezia, R.; Mezzetti, A. The Unique Photophysical Properties of Peridinin-Chlorophyll-a Protein. *Curr. Protein Pept. Sci.* **2014**, *15*, 332–350.
- (4) Schulte, T.; Johanning, S.; Hofmann, E. Structure and Function of Native and Refolded Peridinin-Chlorophyll-Proteins from Dinoflagellates. *Eur. J. Cell Biol.* **2010**, *89*, 990–997.
- (5) Polivka, T.; Hiller, R. G.; Frank, H. A. Spectroscopy of the Peridinin-Chlorophyll a Protein: Insight into Light-Harvesting Strategy of Marine Algae. *Arch. Biochem. Biophys.* **2007**, *458*, 111–120.
- (6) Afar, B.; Merrill, J.; Clark, E. A. Detection of Lymphocyte Subsets using Three-Color/Single Laser Flow Cytometry and the Fluorescent Dye Peridinin-Chlorophyll-a-Protein. *J. Clin. Immunol.* **1991**, *11*, 254–261.
- (7) Mackowski, S. Hybrid Nanostructures for Efficient Light Harvesting. *J. Phys.: Condens. Matter* **2010**, *22*, 193102–193119.
- (8) Zigmantas, D.; Hiller, R. G.; Yarsev, A.; Sundstrom, V.; Polivka, T. Dynamics of Excited States of the Carotenoid Peridinin in Polar Solvents: Dependence on Excitation Wavelength, Viscosity, and Temperature. *J. Phys. Chem. B* **2003**, *107*, 5339–5348.
- (9) Frank, H. A.; Bautista, J. A.; Jusue, J.; Pendon, Z.; Hiller, R. G.; Sharples, P. P.; Gostzola, D.; Wasielewski, M. R. Effect of the Solvent Environment on the Spectroscopic Properties and Dynamics of the Lowest Excited States of Carotenoids. *J. Phys. Chem. B* **2000**, *104*, 4569–4577.
- (10) Wagner, N. L.; Greco, J. A.; Enriquez, M. M.; Frank, H. A.; Birge, R. R. The Nature of the Intramolecular Charge Transfer State in Peridinin. *Biophys. J.* **2013**, *104*, 1314–1325.
- (11) Bonetti, C.; Alexandre, M. T. A.; van Stokkum, I. H. M.; Hiller, R. G.; Groot, M. L.; van Grondelle, R.; Kennis, J. T. M. Identification of an Excited-State Energy Transfer and Relaxation Pathways in the Peridinin-Chlorophyll Complex: An Ultrafast Mid-Infrared Study. *Phys. Chem. Chem. Phys.* **2010**, *12*, 9256–9266.
- (12) Mezzetti, A.; Spezia, R. Time-Resolved Step-Scan FTIR Spectroscopy and DFT Investigation on Triplet Formation in Peridinin-Chlorophyll-a-Protein from Amphidinium Carterae at Low Temperature. *Spectrosc. Int. J.* **2008**, *22*, 235–250.
- (13) Van Tasse, A. J.; Prantil, M. A.; Hiller, R. G.; Fleming, G. R. Excited-State Structural Dynamics of the Charge Transfer state of Peridinin. *Isr. J. Chem.* **2007**, *47*, 17–24.
- (14) Bonetti, C.; Alexandre, M. T. A.; Hiller, R. G.; Kennis, J. T. M.; van Grondelle, R. Chl-a Triplet Quenching by Peridinin in H-PCP and Organic Solvent Revealed by Step-Scan FTIR Time-Resolved Spectroscopy. *Chem. Phys.* **2009**, *357*, 63–69.
- (15) Alexandre, M. T. A.; Luhrs, D. C.; van Stokkum, I. H. M.; Hiller, R.; Groot, M. L.; Kennis, J. T. M.; van Grondelle, R. Triplet State Dynamics in Peridinin-Chlorophyll a Protein: A New Pathway of Photoprotection in LHCs? *Biophys. J.* **2007**, *93*, 2118–2128.
- (16) Bovi, D.; Mezzetti, A.; Vuilleumier, R.; Gaigeot, M.-P.; Chazallon, B.; Spezia, R.; Guidoni, L. Environmental Effects on Vibrational Properties of Carotenoids: Experiments and Calculations on Peridinin. *Phys. Chem. Chem. Phys.* **2011**, *13*, 20954–20964.
- (17) Alexandre, M.; van Grondelle, R. Time-Resolved FTIR Difference Spectroscopy Reveals the Structure and Dynamics of Carotenoid and Chlorophyll Triplets in Photosynthetic Light-Harvesting Complexes. In *Infrared Spectroscopy: Life and Biomedical Sciences*; Theophanides, T., Ed.; InTech: Rijeka, Croatia, 2012; pp 231–256.
- (18) Robert, B. Resonance Raman Studies of Bacterial Reaction Centers. *Biochim. Biophys. Acta, Bioenergetics* **1990**, *1017*, 99–111.
- (19) Martinson, T. A.; Plumley, F. G. One-Step Extraction and Concentration of Pigments and Acyl Lipids from *in vitro* and *in vivo* Samples. *Anal. Biochem.* **1995**, *228*, 123–130.
- (20) Neese, F. ORCA, an *ab initio*, DFT and Semiempirical Electronic Structure Package, version 2.9, Max-Planck-Institut für Chemische Energiekonversion: München, Germany, 2000, unpublished.
- (21) Neese, F. Approximate Second-Order SCF Convergence for Spin Unrestricted Wavefunctions. *Chem. Phys. Lett.* **2000**, *325*, 93–98.
- (22) Perdew, J.; Burke, K.; Ernzerhof, M. Generalized Gradient Approximation Made Simple. *Phys. Rev. Lett.* **1996**, *77*, 3865–3868.
- (23) Schäfer, A.; Horn, H.; Ahlrichs, R. Fully-Optimized Contracted Gaussian-Basis Sets for Atoms Li to Kr. *J. Chem. Phys.* **1992**, *97*, 2571–2577.
- (24) Sinnecker, S.; Rajendran, A.; Klamt, A.; Diedenhofen, M.; Neese, F. Calculation of Solvent Shifts on Electronic g-Tensors with the Conductor-Like Screening Model (COSMO) and its Self-

Consistent Generalization to Real Solvents (Direct COSMO-RS). *J. Phys. Chem. A* **2006**, *110*, 2235–2245.

(25) Saito, S.; Tasumi, M. Normal-Coordinate Analysis of β -Carotene Isomers and Assignments of the Raman and Infrared Bands. *J. Raman Spectrosc.* **1983**, *14*, 310–321.

(26) Robert, B. Resonance Raman Spectroscopy. *Photosynth. Res.* **2009**, *101*, 147–155.

(27) Robert, B. The Electronic Structure, Stereochemistry and Resonance Raman Spectroscopy of Carotenoids. In: *The photochemistry of Carotenoids*. Frank, H. A.; Young, A. J.; Britton, G.; Cogdell, R. J., Eds.; Kluwer Academic Publisher: Dordrecht, The Netherlands, 1999; pp 189–201.

(28) Koyama, Y.; Takatsuka, I.; Nakata, M.; Tasumi, M. Raman and Infra-Red Spectra of the all-*trans*, 7-*cis*, 9-*cis*, 13-*cis* and 15-*cis* Isomers of β -Carotene: Key Bands Distinguishing Stretched or Terminal Bent Configurations from Central-Bent Configurations. *J. Raman Spectrosc.* **1988**, *19*, 37–49.

(29) Jones, R. N.; Angell, C. L.; Ito, T.; Smith, R. J. D. The Carbonyl Stretching Bands in the Infrared Spectra of Unsaturated Lactones. *Can. J. Chem.* **1959**, *37*, 2007–2022.

(30) Nymqvist, R. A.; Fouchea, H. A.; Hoffman, G. A.; Hasha, D. L. Infrared Study of β -Propiolactone in Various Solvent Systems and Other Lactones. *Appl. Spectrosc.* **1991**, *45*, 860–867.

(31) Bond, R. P. M.; Cairns, T.; Connolly, J. D.; Eglinton, G.; Overton, K. H. Infrared Studies with Terpenoid Compounds. Part II. Carbonyl Absorption of γ -Lactones. *J. Chem. Soc.* **1965**, 3958–3963.

(32) Jones, R. N.; Gallagher, B. S. The Infrared Spectra of Steroid Lactones. *J. Am. Chem. Soc.* **1959**, *81*, 5242–5251.

(33) Winston, A.; Kemper, R. N. The Split Carbonyl Band in the Infrared Spectra of Halogen Derivatives of 4-hydroxy-2,4-pentadienoic Acid Lactone. *Tetrahedron* **1971**, *27*, 543–548.

(34) In ref 33, different from refs 29 and 31, it is suggested that the vibrational mode going in Fermi resonance with the lactonic C=O of butenolide compounds is a symmetric–asymmetric coupling of the C–O and C–C bonds of the O=C–C group. This is possibly also the origin of the Fermi resonance we suggest is taking place in Per. We underline that the basic model used in the present paper, involving a “solvent insensitive” band which undergoes Fermi resonance coupling with a solvent-sensitive C=O band still holds true in such an hypothesis.

(35) Fermi, E. Über den Ramaneffekt des Kohlendioxyds. *Z. Phys.* **1931**, *71*, 250–259.

(36) Heller, E. J. Wigner Phase Space Method: Analysis for Semiclassical Applications. *J. Chem. Phys.* **1976**, *65*, 1289–1298.

(37) Allen, M. P.; Tildesley, D. J. *Computer Simulations of Liquids*; Oxford University Press: Oxford, 1987.

(38) Yoshida, T.; Maoka, T.; Das, S. K.; Kanazawa, K.; Horinaka, M.; Wakada, M.; Satomi, H.; Nishino, H.; Sakai, T. Halocynthiaxanthin and Peridin Sensitize Colon Cancer Cells to Tumor Necrosis Factor-Related Apoptosis-Inducing Ligand. *Mol. Cancer Res.* **2007**, *5*, 615–625.

(39) Kupchan, S. M.; Giacobbe, T. J.; Krull, I. S.; Thomas, A. M.; Eakin, M. A.; Fessler, D. C. Reaction of Endocyclic $\alpha\beta$ Unsaturated γ -Lactones with Thiols. *J. Org. Chem.* **1970**, *35*, 3539–3543.

(40) Johansen, J. E.; Svec, W. A.; Liaaen-Jensen, S. Carotenoids on the *Dinophyceae*. *Phytochemistry* **1974**, *13*, 2261–2271.